



# Hyaluronidase Impairs Neutrophil Function and Promotes Group B *Streptococcus* Invasion and Preterm Labor in Nonhuman Primates

Michelle Coleman,<sup>a</sup>  Blair Armistead,<sup>a,b</sup> Austyn Orvis,<sup>a</sup> Phoenicia Quach,<sup>a</sup> Alyssa Brokaw,<sup>a,b</sup> Claire Gendrin,<sup>a</sup> Kavita Sharma,<sup>a</sup> Jason Ogle,<sup>c</sup> Sean Merillat,<sup>a</sup> Matthew Dacanay,<sup>d</sup> Tsung-Yen Wu,<sup>d</sup> Jeff Munson,<sup>e</sup> Audrey Baldessari,<sup>c</sup> Jay Vornhagen,<sup>a,b\*</sup> Anna Furuta,<sup>a,b</sup> Shayla Nguyen,<sup>a</sup>  Kristina M. Adams Waldorf,<sup>b,d,f,g</sup>  Lakshmi Rajagopal<sup>a,b,f,h</sup>

<sup>a</sup>Center for Global Infectious Disease Research, Seattle Children's Research Institute, Seattle, Washington, USA

<sup>b</sup>Department of Global Health, University of Washington, Seattle, Washington, USA

<sup>c</sup>Washington National Primate Research Center, Seattle, Washington, USA

<sup>d</sup>Department of Obstetrics and Gynecology, University of Washington School of Medicine, Seattle, Washington, USA

<sup>e</sup>Department of Psychiatry and Behavioral Sciences, University of Washington, Seattle, Washington, USA

<sup>f</sup>Center for Innate Immunity and Immune Disease, University of Washington, Seattle, Washington, USA

<sup>g</sup>Sahlgrenska Academy, University of Gothenburg, Gothenburg, Sweden

<sup>h</sup>Department of Pediatrics, University of Washington, Seattle, Washington, USA

Michelle Coleman and Blair Armistead contributed equally to this article. Author order was determined by seniority.

**ABSTRACT** Invasive bacterial infections during pregnancy are a major risk factor for preterm birth, stillbirth, and fetal injury. Group B streptococci (GBS) are Gram-positive bacteria that asymptotically colonize the lower genital tract but infect the amniotic fluid and induce preterm birth or stillbirth. Experimental models that closely emulate human pregnancy are pivotal for the development of successful strategies to prevent these adverse pregnancy outcomes. Using a unique nonhuman primate model that mimics human pregnancy and informs temporal events surrounding amniotic cavity invasion and preterm labor, we show that the animals inoculated with hyaluronidase (HylB)-expressing GBS consistently exhibited microbial invasion into the amniotic cavity, fetal bacteremia, and preterm labor. Although delayed cytokine responses were observed at the maternal-fetal interface, increased prostaglandin and matrix metalloproteinase levels in these animals likely mediated preterm labor. HylB-proficient GBS dampened reactive oxygen species production and exhibited increased resistance to neutrophils compared to an isogenic mutant. Together, these findings demonstrate how a bacterial enzyme promotes GBS amniotic cavity invasion and preterm labor in a model that closely resembles human pregnancy.

**IMPORTANCE** Group B streptococci (GBS) are bacteria that commonly reside in the female lower genital tract as asymptomatic members of the microbiota. However, during pregnancy, GBS can infect tissues at the maternal-fetal interface, leading to preterm birth, stillbirth, or fetal injury. Understanding how GBS evade host defenses during pregnancy is key to developing improved preventive therapies for these adverse outcomes. In this study, we used a unique nonhuman primate model to show that an enzyme secreted by GBS, hyaluronidase (HylB) promotes bacterial invasion into the amniotic cavity and fetus. Although delayed immune responses were seen at the maternal-fetal interface, animals infected with hyaluronidase-expressing GBS exhibited premature cervical ripening and preterm labor. These observations reveal that HylB is a crucial GBS virulence factor that promotes bacterial invasion and preterm labor in a pregnancy model that closely emulates human pregnancy. Therefore, hyaluronidase inhibitors may be useful in therapeutic strategies against ascending GBS infection.

**Citation** Coleman M, Armistead B, Orvis A, Quach P, Brokaw A, Gendrin C, Sharma K, Ogle J, Merillat S, Dacanay M, Wu T-Y, Munson J, Baldessari A, Vornhagen J, Furuta A, Nguyen S, Adams Waldorf KM, Rajagopal L. 2021. Hyaluronidase impairs neutrophil function and promotes group B *Streptococcus* invasion and preterm labor in nonhuman primates. *mBio* 12: e03115-20. <https://doi.org/10.1128/mBio.03115-20>.

**Editor** Carolyn B. Coyne, University of Pittsburgh School of Medicine

**Copyright** © 2021 Coleman et al. This is an open-access article distributed under the terms of the [Creative Commons Attribution 4.0 International license](https://creativecommons.org/licenses/by/4.0/).

Address correspondence to Kristina M. Adams Waldorf, [adamsk@uw.edu](mailto:adamsk@uw.edu), or Lakshmi Rajagopal, [lakshmi.rajagopal@seattlechildrens.org](mailto:lakshmi.rajagopal@seattlechildrens.org).

\* Present address: Jay Vornhagen, University of Michigan, Ann Arbor, Michigan, USA.

**Received** 2 November 2020

**Accepted** 9 November 2020

**Published** 5 January 2021

**KEYWORDS** group B streptococcus, hyaluronidase, immune evasion, neutrophils, pregnancy, preterm labor

Globally, invasive bacterial infections are a leading cause of stillbirth and preterm birth (1–3). Group B streptococci (GBS) or *Streptococcus agalactiae* are beta-hemolytic, Gram-positive bacteria that commonly exist as commensal organisms in the rectovaginal tracts of healthy adult women. However, GBS can be transmitted to neonates during birth or ascend into the uterus during pregnancy, resulting in fetal injury, stillbirth, preterm birth, or early neonatal infection (4–6). Recent reports have indicated that by conservative estimates, approximately 147,000 stillbirths and 3.5 million preterm births each year are attributed to GBS infections (7). Currently, there are no therapies to prevent preterm birth or stillbirth. Some countries have implemented protocols to screen women for GBS colonization in the third trimester of pregnancy and to subsequently administer antibiotics to GBS-positive women during labor and delivery (known as intrapartum antibiotic prophylaxis). Although these measures have decreased the incidence of neonatal GBS disease in the first week of life (8, 9), they fail to prevent adverse pregnancy outcomes that occur prior to labor and delivery that result in preterm births or stillbirths (8, 10–12).

Improved preventive therapies for GBS require a greater understanding of the complex interactions between pathogen and host. One host factor important for responses to microbial infection is hyaluronan (HA). HA is a major constituent of the host extracellular matrix and exists as a high-molecular-weight glucosaminoglycan polymer that assists in cell migration, cell-cell signaling, and responses to injury and infection (13, 14). During infection or injury, high-molecular-weight HA (HMW-HA) is degraded by host hyaluronidases or reactive oxygen species (ROS) to low-molecular-weight HA (LMW-HA; comprising HA tetramers or pentamers), which are proinflammatory in nature and mediate cytokine responses through signaling via Toll-like receptors (TLRs), such as TLR-2 and TLR-4 (15, 16). Interestingly, certain bacterial pathogens such as GBS also secrete a hyaluronidase enzyme (17, 18). The GBS hyaluronidase (HylB; encoded by the *hylB* gene) was identified in 1950 as an exolytic enzyme (19) that breaks down HA into disaccharide fragments (20). Recently, GBS HylB-generated HA disaccharides were shown to block TLR-2 and TLR-4 signaling in macrophages and dampen cytokine responses (21). Subsequently, we observed that clinical GBS isolates associated with women in preterm labor or neonatal infections exhibit increased hyaluronidase activity compared to commensal GBS isolates obtained from rectovaginal swabs of healthy women (22). We also noted that GBS hyaluronidase dampened uterine immune responses and postulated that these promoted ascending infection in a pregnant mouse model of GBS infection (22).

However, the pregnant mouse and other lower mammalian models exhibit dissimilarities to many aspects of human pregnancy, including differences in reproductive anatomy, placentation, onset of labor, and sensitivity to pathogens. In contrast, the closest animal model for studies related to human pregnancy is the pregnant nonhuman primate (NHP) (23–26). Similarities of NHPs to humans include reproductive anatomy, type and structure of placenta (hemomonochorial), number of fetuses (singleton), long gestational period (160 to 170 days), initiation of labor (hormonal control of parturition), sensitivity to pathogens, and the developmental timeline of the fetal lung and brain (25, 26). In the chronically catheterized pregnant NHP model (27, 28), we inoculate bacteria at the choriodecidual space, a site in the pregnant uterine mucosa between the uterine muscle and the placental membranes, where bacteria are thought to first encounter the maternal-fetal interface during ascending infection from the lower genital tract (2, 27).

Here, we used a nonhemolytic GBS strain (serotype V, GB37) that exhibits increased hyaluronidase activity (29) to address how hyaluronidase contributes to immune evasion, fetal injury, and preterm labor. We found that pregnant NHPs inoculated with GB37 exhibited rapid microbial invasion of the amniotic cavity, fetal bacteremia, and

preterm labor in contrast to animals inoculated with the isogenic, hyaluronidase-deficient strain. Analyses of the cellular and biochemical events at the maternal-fetal interface revealed impaired host defenses that likely prompted the early onset of labor. Together, our studies show that a bacterial hyaluronidase promotes microbial invasion of the amniotic cavity and preterm labor in the nonhuman primate model.

## RESULTS

**HyIB promotes adverse pregnancy outcomes in an NHP model of choriodecidual GBS infection.** To elucidate whether hyaluronidase promotes GBS infection and adverse outcomes during pregnancy, we used a chronically catheterized nonhuman primate (*Macaca nemestrina*) model that closely emulates human pregnancy and defines temporal events during amniotic cavity invasion and preterm labor (28). Ten animals received choriodecidual inoculations of  $1 \times 10^8$  to  $3 \times 10^8$  CFU of either hyaluronidase-proficient wild-type GBS (strain GB37,  $n = 5$ ) or an isogenic hyaluronidase-deficient GBS (strain GB37 $\Delta$ hyIB,  $n = 5$ ). Controls included NHPs that received saline ( $n = 6$  total;  $n = 4$  were described previously [27]). Adverse pregnancy outcomes, specifically preterm labor and/or microbial invasion of the amniotic cavity (Table 1) were the primary outcomes of our study. In GBS-inoculated animals, Cesarean section was performed at the onset of preterm labor, which was defined as progressive cervical dilation associated with increased and sustained uterine activity or at 3 days post-GBS inoculation if preterm labor did not occur, as described previously (28).

We found that choriodecidual inoculation of the hyaluronidase-proficient GBS strain (GB37) induced preterm labor in 4/5 (80%) animals compared to 1/5 (20%) animals inoculated with the isogenic hyaluronidase-deficient strain GB37 $\Delta$ hyIB or 0/6 (0%) saline controls (Table 1 and Fig. 1). Further, all GB37-inoculated animals (5/5, 100%) experienced microbial invasion of the amniotic cavity in contrast to 1/5 animals (20%) inoculated with GB37 $\Delta$ hyIB and 0/6 (0%) saline controls (Table 1 and Fig. 1). In the GB37 group, GBS CFU was recovered from the amniotic fluid (AF) as early as 6 h postinoculation in three animals (GB37#1, GB37#2, and GB37#4), which was followed by preterm labor within 1 and 2 days (Fig. 1; see also Fig. S1 in the supplemental material). For GB37#3, GBS bacteria was recovered from the AF by 12 h after inoculation, and the AF was significantly turbid due to high bacterial burden within day 2. This was accompanied by a heavy uterine contraction pattern that resulted in cervical ripening (softening). To avoid a stillbirth due to sepsis, we proceeded with Cesarean section at 49 h after GBS inoculation for this animal. In GB37#5, infection and contractions progressed rapidly after 48 h, and the NHP was in labor by 70 h (early on day 3). In the GB37 $\Delta$ hyIB group, only one animal exhibited preterm labor and microbial invasion of the amniotic cavity (GB37 $\Delta$ hyIB#5), wherein GBS was detected in the AF at 24 h postinoculation and the animal experienced preterm labor within 70 h (Fig. 1; see also Fig. S1). The remaining four animals in this group did not exhibit microbial invasion of the amniotic cavity, preterm labor, or other adverse outcomes (Fig. 1; see also Fig. S1). Collectively, our results indicate that choriodecidual inoculation of a GBS strain with elevated hyaluronidase activity was significantly associated with adverse pregnancy outcomes compared to inoculation with the isogenic hyaluronidase-deficient GBS strain or saline controls ( $P = 0.02$  GB37 versus GB37 $\Delta$ hyIB;  $P = 0.0005$  GB37 versus saline). Despite the significant adverse outcomes noted in the GB37-infected group, there was no statistical difference in the peak AF cytokine levels among the three treatment groups of this study (i.e., saline, GB37, and GB37 $\Delta$ hyIB; Table 1). Interestingly, compared to our previously published studies on hyperhemolytic GBS $\Delta$ covR-inoculated animals (28), where we reported peak AF interleukin-6 (IL-6) and IL-8 ranging between 15 and 22 ng/ml (for animals with microbial invasion of the amniotic cavity), the GB37 group had significantly lower peak AF levels of IL-6 ( $P = 0.009$ ) and IL-8 ( $P = 0.02$ ). Taken together, these results suggest that increased AF cytokines such as IL-6 and IL-8 are not necessarily a predictive signature of preterm labor, particularly during infection with the immunosuppressive hyaluronidase-expressing GBS bacteria.

**TABLE 1** Summary of pregnancy outcomes, cytokines, and prostaglandins in pregnant NHPs<sup>a</sup>

Outcome	P					
	Saline (n = 6)	GB37 (n = 5)	GB37Δhy/B (n = 5)	Saline vs GB37	GB37 vs GB37Δhy/B	Saline vs GB37Δhy/B
Primary and composite outcomes, no. (%)						
Adverse outcome <sup>b</sup>	0 (0)	5 (100)	1 (20)	<b>0.0009</b>	<b>0.02</b>	NS
Preterm labor <sup>c</sup>	0 (0)	4 (80)	1 (20)	<b>0.01</b>	0.1	NS
Microbial invasion of the amniotic cavity and fetal bacteremia	0 (0)	5 (100)	1 (20)	<b>0.0009</b>	<b>0.02</b>	NS
Peak contractions, AF cytokines, and prostaglandins, mean peak pg/ml (SEM)						
Hourly contraction area	1,326.7 (506.58)	5,606.0 (1,165.1)	3,087.4 (1,050.0)	<b>0.04</b>	NS	NS
IL-1β	31.61 (20.59)	1,754.8 (1,112.7)	597.65 (583.42)	0.09	NS	NS
TNF-α	26.13 (11.44)	574.58 (285.82)	97.58 (39.43)	0.07	NS	NS
IL-6	7,091.1 (2,642.2)	2,827.8 (1,331.3)	2,404.1 (1,356.5)	NS	NS	NS
IL-8	888.07 (321.53)	2,120.5 (1,383.3)	1,629.7 (1,498.2)	NS	NS	NS
PGE <sub>2</sub>	509.83 (247.84)	1,160.9 (647.40)	289.23 (116.69)	NS	NS	NS
PGF <sub>2α</sub>	424.31 (169.64)	1,808.1 (887.27)	164.93 (45.91)	NS	0.08	NS
Fetal cytokines						
IL-1β	0.80 (0.60)	2.152 (0.8584)	1.128 (0.8645)	NS	NS	NS
TNF-α	2.268 (1.127)	0.01 (0.0)	0.01 (0.0)	<b>0.04</b>	NS	<b>0.04</b>
IL-6	3.639 (1.852)	1,049.6 (722.10)	44.74 (41.58)	<b>0.049</b>	NS	NS
IL-8	574.06 (314.04)	2,648.8 (1,674.1)	2,576.2 (1,551.3)	NS	NS	NS

<sup>a</sup>The primary outcomes are shown as "number (%)" and were compared among groups using Barnard's test. Amniotic fluid (AF) cytokines, prostaglandins and fetal plasma cytokines are expressed as mean peak (SEM) in pg/ml. Hourly contraction area is expressed in mm Hg × s/h. Cytokines (IL-1β, TNF-α, IL-6, and IL-8) and prostaglandins (PGE<sub>2</sub> and PGF<sub>2α</sub>) were compared by using one-way ANOVA with Bonferroni's correction. Statistical analyses were conducted using Intercooled STATA 8.2 for Windows 2000 (StataCorp) or SciStatCalc. P values of <0.05 are indicated in boldface. NS, P > 0.100.

<sup>b</sup>Adverse outcome is a composite metric representing preterm labor or microbial invasion of the amniotic cavity with fetal bacteremia.

<sup>c</sup>Preterm labor was defined as progressive cervical dilation associated with increased and sustained uterine activity.

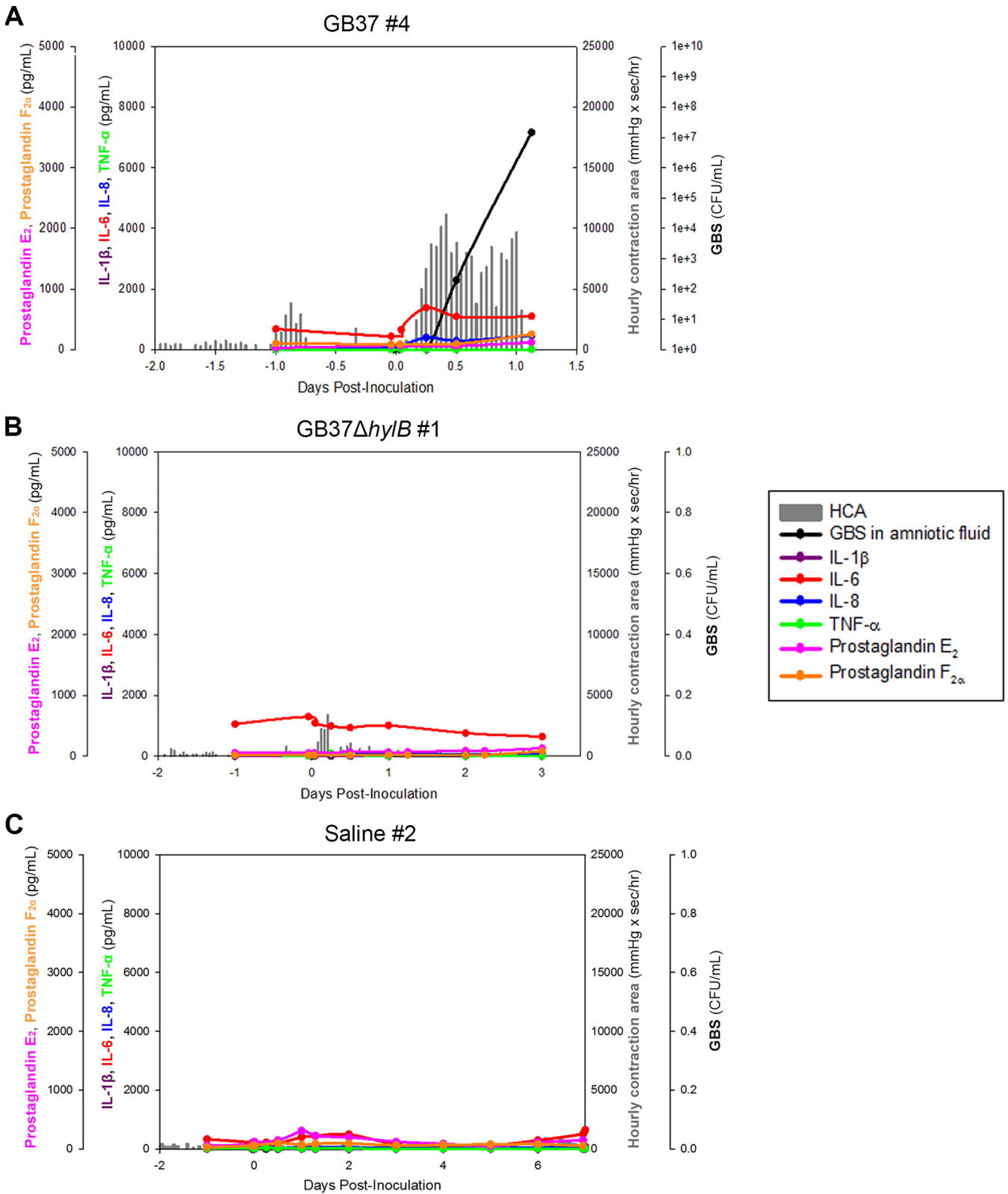


**FIG 1** GBS hyaluronidase promotes amniotic cavity invasion and preterm labor. Chronically catheterized pregnant pigtail macaques (*Macaca nemestrina*) received choriondecidual inoculations of either HyIB-proficient WT GBS strain GB37 ( $n=5$ ), an isogenic GBS strain lacking HyIB (GB37 $\Delta$ hyIB,  $n=5$ ), or saline ( $n=6$ ) at 118 to 125 days gestation (term, 172 days). Uterine contractions (vertical gray lines), cytokines (IL-1 $\beta$ , IL-6, IL-8, and tumor necrosis factor alpha [TNF- $\alpha$ ]), prostaglandins (PGE<sub>2</sub> and PGF<sub>2 $\alpha$</sub> ), and GBS CFU from the AF are shown from representative animals that received either GB37 (A), GB37 $\Delta$ hyIB (B), or saline (C).

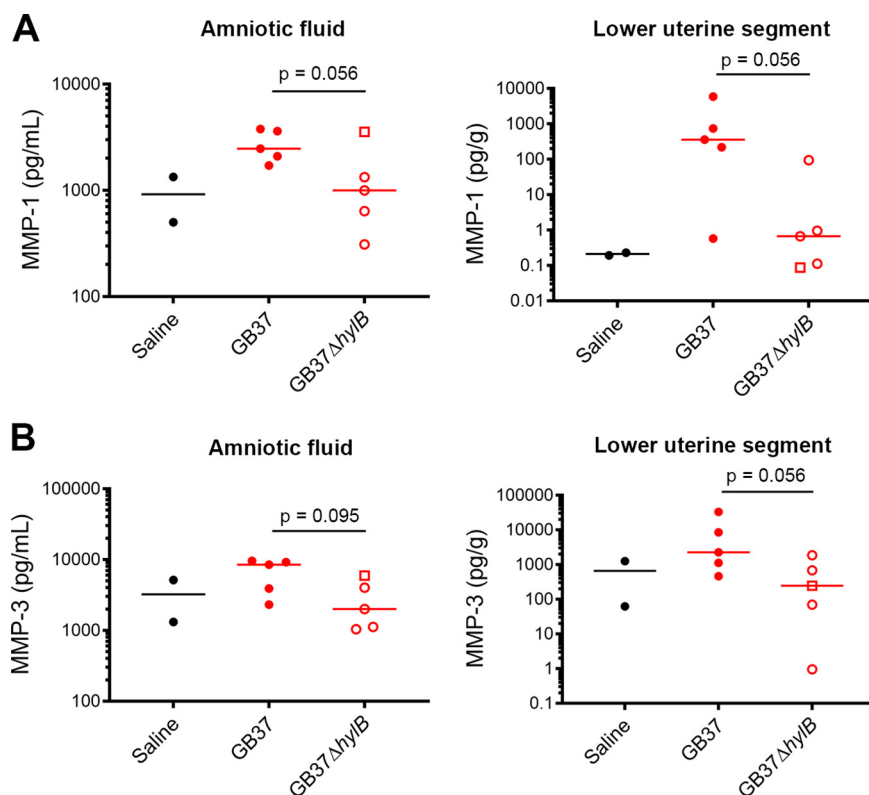


**FIG 2** MMP-1 and MMP-3 are elevated in the amniotic fluid and lower uterus of GB37-inoculated NHP. At Cesarean section, amniotic fluid and a tissue segment from the lower uterus were collected from each animal, and each sample was analyzed for MMP-1 (A) and MMP-3 (B) levels by Luminex. Data from GB37 and GB37ΔhyIB were compared using a Mann-Whitney test. Although *P* values between 0.055 and 0.1 are noted due to the small sample size of this nonhuman primate study, *P* values of <0.05 were considered significant. GB37ΔhyIB#5 is designated by an open square.

**GBS HyIB promotes prostaglandin and matrix metalloproteinase synthesis for cervical softening.** Apart from increased inflammation, prostaglandin and matrix metalloproteinases (MMPs) have been implicated in inducing the thinning and softening of the cervix, leading to preterm labor (30–33). Given our observations that 80% (4/5) of the GB37-infected animals experienced preterm labor in the setting of low inflammation, we sought to determine whether infection with the hyaluronidase-proficient GBS was associated with increased prostaglandin and MMP levels, which could have contributed to cervical softening and preterm labor. We observed a relative increase in MMP-1 and MMP-3 in the AF and lower uterine segments of GB37 animals compared to GB37ΔhyIB or saline controls (Fig. 2; see the schematic in Fig. S4a in the supplemental material for the location of the lower uterine segment). These MMPs have been implicated in preterm labor (34, 35). We also noted that peak AF prostaglandin PGF2α levels were higher in the GB37 animals compared to GB37ΔhyIB (Table 1). Together, these data provide some potential insight into mechanisms of preterm labor due to infection by the immunosuppressive hyaluronidase-expressing GBS.

**GBS HyIB promotes fetal bacteremia and fetal inflammation.** In all GB37-infected animals, microbial invasion of the amniotic cavity coincided with fetal bacteremia, and GBS CFU (ranging from 10<sup>3</sup> to 10<sup>8</sup> CFU/g) were recovered from several fetal organs, including the lung, spleen, heart, brain, and meninges (Fig. 3A). In the GB37ΔhyIB group, only the animal that exhibited microbial invasion of the amniotic cavity (GB37ΔhyIB#5) exhibited fetal bacteremia. Overall, fetal bacteremia was significantly increased in animals inoculated with GB37 compared to GB37ΔhyIB (Fig. 3A) with

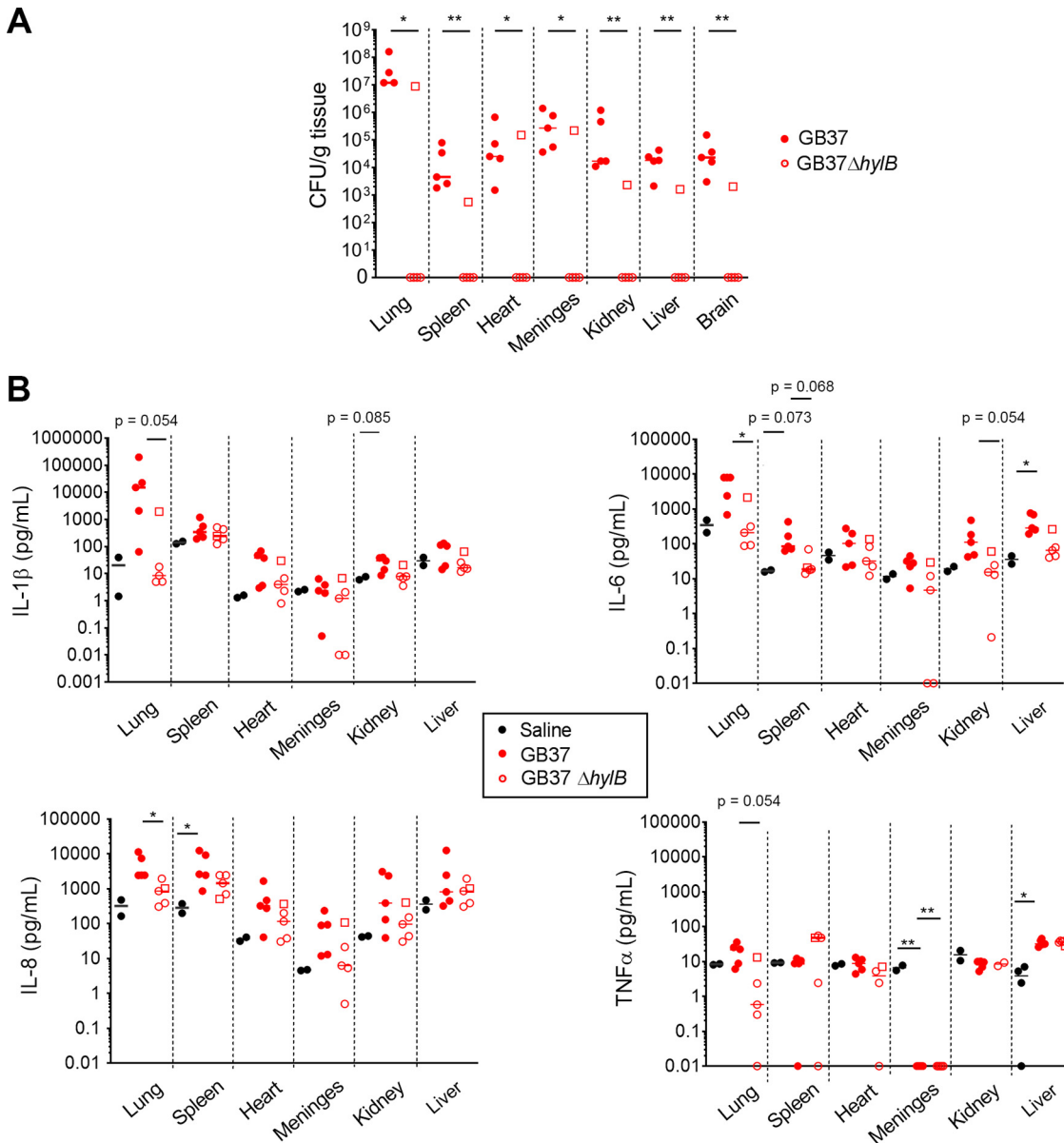


**FIG 3** Microbial invasion of the amniotic cavity coincided with fetal bacteremia and systemic fetal inflammation. At Cesarean section, fetal tissues were harvested from chronically catheterized pregnant NHP that received a chorioamniotic inoculation of saline, GB37, or GB37 $\Delta$ hylB. GB37 $\Delta$ hylB#5 is designated by an open square. (A) Numbers of GBS CFU obtained from various fetal tissues. Note that GBS was recovered from all fetal tissues of all animals that experienced microbial invasion of the amniotic cavity and preterm birth, including all (5/5) GB37-inoculated animals and one of five GB37 $\Delta$ hylB-inoculated animals (GB37 $\Delta$ hylB#5, designated by an open square). Differences in CFU between treatment groups were analyzed using the Mann-Whitney test. \*,  $P < 0.05$ ; \*\*,  $P < 0.01$ . (B) Lysates from fetal tissues were examined by Luminex to evaluate differences in levels of fetal cytokines. A Kruskal-Wallis test with Dunn's multiple-comparison test was performed. \*,  $P < 0.05$ .  $P$  values between 0.05 and 0.1 are noted due to the small sample size of this nonhuman primate study but were not considered significant. Since fetal tissue lysates were not available from historical saline animals ( $n=4$ ) reported previously (28), only saline animals performed in the present study ( $n=2$ ) were included in these analyses.

consistently more bacteria recovered from the fetal lung compared to the other fetal organs.

We also measured cytokines in fetal plasma and tissues from samples obtained at the study endpoint (Fig. 3B and Table 1). In contrast to low levels of proinflammatory cytokines observed in the amniotic fluid, we noted significantly increased cytokines in the fetal lung (IL-8), spleen (IL-8), and liver (IL-6) when comparing GB37-infected

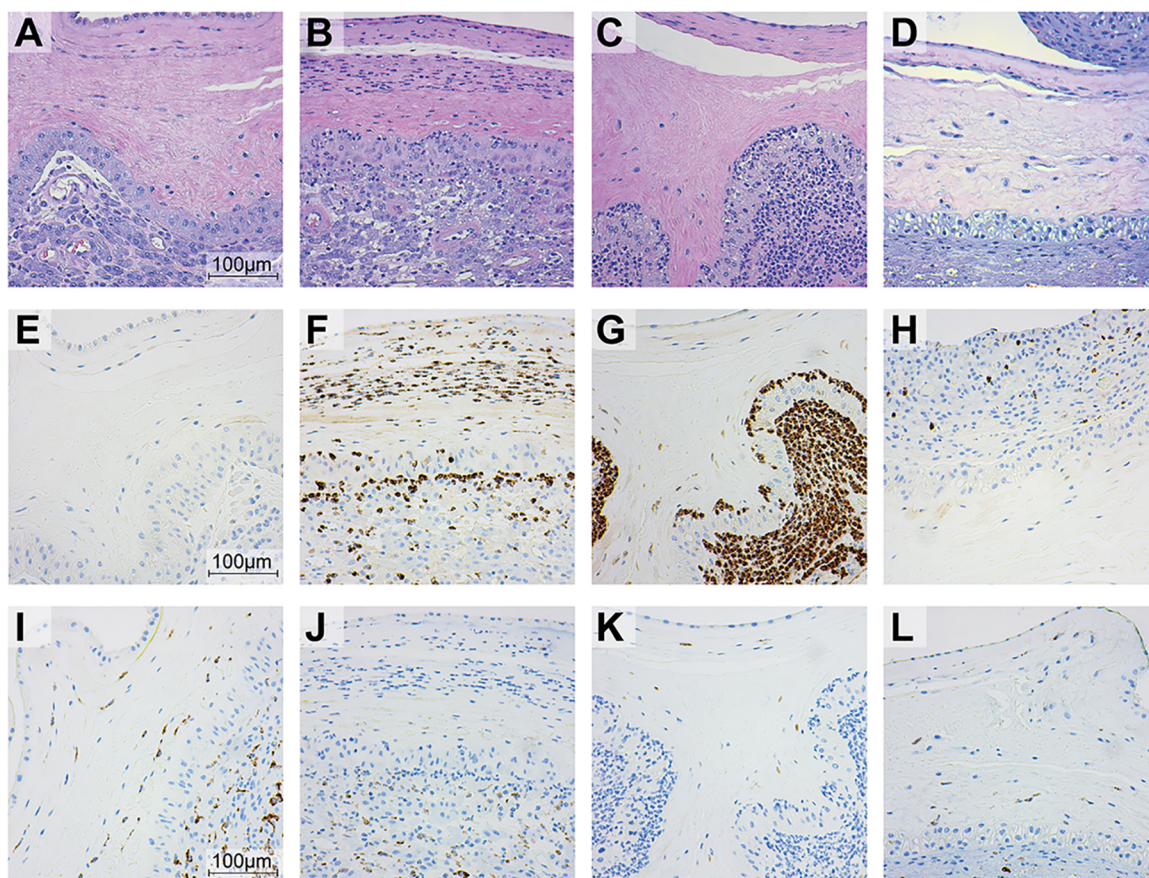


**FIG 4** Histological examination of the placental membranes revealed increased neutrophil infiltration in GB37-infected animals. (A to D) H&E staining of NHP placental sections. Representative H&E-stained sections from NHPs in each group are shown, including saline#3 (A), GB37#1 (B), GB37#2 (C), and GB37 $\Delta$ hyIB#2 (D). (E to H) Representative MPO-stained sections from NHPs in each group, including saline#3 (E), GB37#1 (F), GB37#2 (G), and GB37 $\Delta$ hyIB#2 (H). (I to L) Representative CD68-stained sections from NHPs in each group, including saline#2 (I), GB37#1 (J), GB37#2 (K), and GB37 $\Delta$ hyIB#2 (L). For the GB37 group, tissues in panels B, F, and J were taken 24 h after inoculation and tissues in panels C, G, and K were harvested 48 h after inoculation.

fetuses to saline controls (Fig. 3B). To determine the specific effect of HyIB, we compared GB37 with GB37 $\Delta$ hyIB group and found significantly higher levels of IL-6 in the lung (Fig. 3B). Hematoxylin and eosin (H&E) staining of neonatal lungs supported these findings. Lungs from the GB37 group showed minimal (GB37#4) and moderate to severe (GB37#1, GB37#2, GB37#3, and GB37#5) pneumonia (see Fig. S2). In contrast, H&E staining of the GB37 $\Delta$ hyIB group showed overall minimal neutrophilic inflammation in the fetal lung (see Fig. S2). The only animal with microbial invasion of the amniotic cavity in this group, GB37 $\Delta$ hyIB#5, exhibited moderate and mixed cell-type inflammation within the lung. Myeloperoxidase (MPO; neutrophil and granulocyte marker) staining was seen in the neonatal lungs of the GB37 group with minimal staining observed in the GB37 $\Delta$ hyIB group and saline controls (see Fig. S2 and S3). Minimal to no CD68 (expressed by monocytes and macrophages) staining was observed for all three groups (see Fig. S2). Collectively, these analyses reveal that chorioamniotic inoculation of hyaluronidase-expressing GBS resulted in bacterial invasion, cytokines, and inflammation in the fetal lung.

**GBS HyIB induced greater infiltration of phagocytes to the maternal-fetal interface.** We examined the chorioamniotic membranes at the inoculation site using H&E, MPO, and CD68 to assess inflammation and tissue injury at the maternal-fetal interface. As expected, saline controls revealed minimal to no neutrophil infiltration (Fig. 4A; see also Fig. S3), whereas chorioamniotic membranes from animals in the GB37 group exhibited moderate to severe neutrophilic inflammation (Fig. 4B and C;



see also Fig. S3). Conversely, placental membranes from the GB37 $\Delta$ hyIB group had minimal infiltration (Fig. 4D; see also Fig. S3), except for GB37 $\Delta$ hyIB#5, which exhibited moderate neutrophilic inflammation (data not shown). In contrast, CD68 staining (a marker for monocytes and macrophages) was similar across all three groups (saline, GB37, and GB37 $\Delta$ hyIB; Fig. 4I to L), indicating that neutrophils rather than macrophages are predominantly recruited to the choriodecidual interface during GBS infections. Notably, we also observed increased neutrophil levels in the chorioamniotic membranes and miduterine muscle by flow cytometry in GB37-treated animals compared to those inoculated with the  $\Delta$ hyIB strain (see Fig. S4). Collectively, these data indicate that immune cells typically involved in the host response to tissue damage and/or pathogen control are increased in the reproductive tissues of animals inoculated with GB37 versus GB37 $\Delta$ hyIB or saline controls.

**Digital spatial profiling of the placenta revealed minimal immune signatures to GBS hyaluronidase.** To obtain greater spatial resolution of the cellular events and signaling cascades occurring at the uterine mucosa, we analyzed paraffin-embedded placental membranes using the GeoMx digital spatial profiling (DSP) platform (NanoString Technologies) (Fig. 5). The DSP scanned whole tissue image shown in Fig. 5A is obtained by stitching together images that are obtained from single Field Of View (FOV); each FOV image has a dimension of 2048 pixel  $\times$  2048 pixel, which equals 665.6  $\mu$ m  $\times$  665.6  $\mu$ m. Regions of interest (ROIs) comprising the decidua, chorion, and amnion in each animal were selected with preferential targeting of areas with GBS (Fig. 5A), and 62 antibody probes coupled to cleavable oligonucleotide tags were hybridized and quantified. Counts were mapped to tissue location to yield a spatially resolved profile of analyte abundance (Fig. 5B). Intriguingly, while GBS was detected in the decidua of all GB37-treated animals (Fig. 5A) and in only one GB37 $\Delta$ hyIB animal, no significant differences in inflammation-associated analytes (e.g., CD45, CD68, STING, CD86, and CD56) were observed between the GBS groups for any tissue type (amnion, chorion, decidua) at these ROIs (Fig. 5B; see also Fig. S5). Conversely, some markers associated with inflammation were significantly lower in GB37 animals compared to saline controls, including the macrophage marker CD14 in the decidua and amnion and CD86 (T cell costimulatory molecule on APCs) in the decidua, chorion, and amnion (Fig. 5B; see also Fig. S6). These data indicate that even in tissues sites where GB37 were detected by fluorescence microscopy (Fig. 5A), some inflammatory markers were dampened relative to baseline. Together, digital spatial profiling showed that chorio-decidual inoculation with GB37 did not induce a remarkable proinflammatory signature in the amnion, chorion, or decidua.

**HyIB promotes resistance to antimicrobial effects of neutrophils.** Given our observations of neutrophil recruitment in the chorioamniotic membranes and uterus of GB37-infected animals (Fig. 4; see also Fig. S4), with minimal proinflammatory events in the placenta (Fig. 5B), we sought to determine whether GBS hyaluronidase plays a role in dampening neutrophil defenses, which are critical in protecting the host against GBS infection (28, 36). We previously observed that hyperhemolytic strains of GBS circumvented the neutrophil response, in part, by inducing neutrophil cell death (28). Here, no significant cell death was observed when fresh adult human neutrophils were treated with GB37 or GB37 $\Delta$ hyIB (Fig. 6A). Given that HA is present on the cell surface of neutrophils (37), we next sought to determine whether HyIB might enable GBS to resist the microbicidal activity of neutrophils. We found neutrophils were less able to kill GB37 compared to GB37 $\Delta$ hyIB (Fig. 6B; see also Fig. S8a), indicating that hyaluronidase enables GBS to subvert this critical host defense.

To understand the mechanisms by which HyIB may facilitate GBS resistance to neutrophil killing, we measured the production of ROS in neutrophils in the presence of hyaluronidase-proficient or deficient GBS using a flow cytometry-based assay (see the supplemental methods [Text S1]). We noted decreased production of ROS in neutrophils exposed to GB37 compared to GB37 $\Delta$ hyIB, demonstrating that HyIB may have blunted the ability of neutrophils to generate ROS (Fig. 6C). This effect was also observed with maternal and fetal neutrophils (see Fig. S8b). Next, we sought to

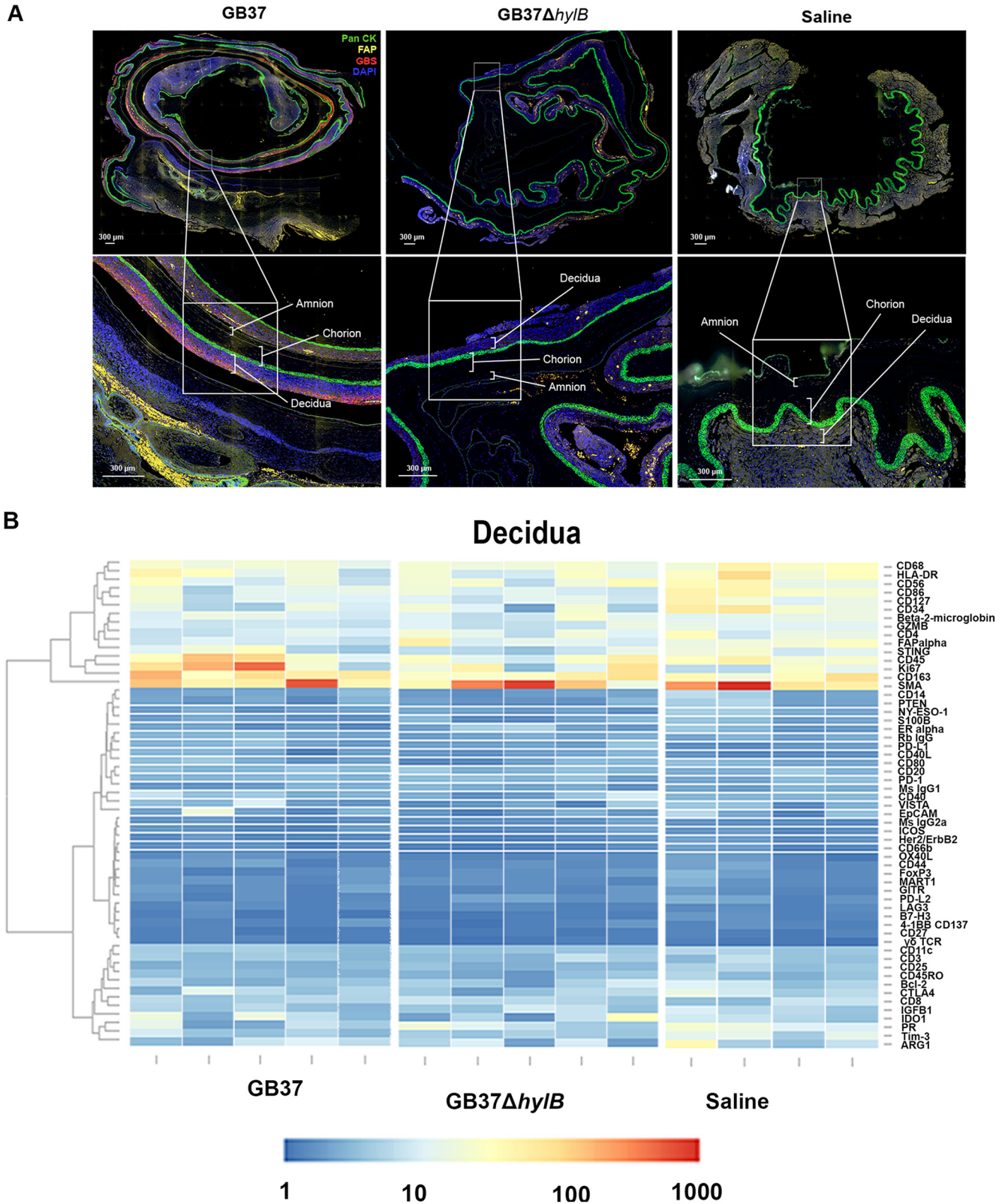


**FIG 5** Digital spatial profiling of placental tissues revealed few differential expressions of immune signatures GBS hyaluronidase. (A) Representative placental sections from NHP in each treatment group (GB37#2, GB37 $\Delta$ hyIB#2, and saline#3). We treated each placental section with fluorescent anti-pan cyokeratin (Pan CK, green), anti-fibronectin attachment protein (FAP, yellow), anti-GBS (red), and DAPI (blue) and then identified the decidua, chorion, and amnion within each section as distinct ROIs. Each discrete ROI (i.e., chorion, amnion, and decidua) was analyzed for analyte abundance. (B) Heatmaps showing analyte abundance (normalized by the signal/noise ratio) in the decidua, chorion, and amnion of each animal in the GB37 ( $n=5$ ), GB37 $\Delta$ hyIB ( $n=5$ ), and saline ( $n=4$ ) groups are shown.



determine whether HylB-mediated TLR-2/4 interference could explain the differences in neutrophil ROS production elicited by the wild-type (WT) and  $\Delta hylB$  strains. To test this, supernatants from GB37 or GB37 $\Delta hylB$  were incubated with HA to allow for enzymatic digestion, as described previously (21). Then, HA digests from each strain were exposed to human neutrophils pretreated with anti-TLR-2 and anti-TLR-4 antibodies or vehicle alone, and ROS production was measured. As expected, GB37-HA digests induced less ROS production than GB37 $\Delta hylB$ -HA digests. Intriguingly, when neutrophils were pretreated with both TLR inhibitors, this effect was lost (Fig. 6D). These findings suggest that proinflammatory HA fragments from hyaluronidase-deficient GBS promote ROS production in neutrophils by engaging TLR-2/4 signaling. Furthermore, these data indicate that GBS may avoid neutrophil killing by using HylB to cleave HA into fragments that blunt TLR2/4 signaling and subsequently diminish ROS production. Taken together, our findings are the first to demonstrate that HylB promotes GBS resistance to neutrophils, which contributes to adverse pregnancy outcomes in pregnant nonhuman primates.

## DISCUSSION

Understanding mechanisms that GBS use to subvert host defenses in its transition from an asymptomatic colonizer to invasive pathogen is essential for the development of improved treatment and prevention strategies for adverse perinatal outcomes associated with GBS. We previously showed that hyaluronidase (HylB) activity was greater in GBS strains isolated from cases of preterm birth and neonatal infection compared to commensal isolates (22) and that HylB facilitated ascending GBS infection in mice (22). Our data in the chronically catheterized NHP model indicate that HylB is a crucial virulence factor that enables GBS to rapidly invade the amniotic cavity and induce preterm labor. Overall, while we noted a relative suppression of inflammation in key placental, uterine, and amniotic fluid samples, preterm labor was induced by HylB-expressing GBS.

Despite clear phenotypic differences in pregnancy outcomes in GB37-treated animals compared to the GB37 $\Delta hylB$  group, differences in peak AF cytokines and immune signaling in the placenta were not as striking. These results are also in stark contrast to a pregnant NHP model using a hyperhemolytic/hyperpigmented GBS strain wherein we observed significantly higher levels of IL-6 and IL-8 in the AF and upregulation of proinflammatory genes in the placenta compared to NHPs inoculated with a nonhemolytic strain and saline controls (28). In contrast, results from this study indicate that HylB may suppress inflammatory responses at the maternal-fetal interface to promote bacterial replication and dissemination. Luminex (Fig. 1), digital spatial profiling (Fig. 5), and *in vitro* studies (Fig. 6), indicate immune suppression, which can be due in part to inhibition of TLR-2/4 signaling by HylB-expressing GBS (Fig. 6D). These data are consistent with observations that term placenta expresses high levels of TLR-2 and TLR-4, with stronger expression of TLR-2 in immune cells and TLR-4 in syncytiotrophoblasts and fibroblasts (38). Expression of TLR-4 was also observed on the apical side of amniotic epithelium (39, 40), suggesting immune suppression of placenta could also occur after microbial invasion of the amniotic cavity. Together, these observations show that immune cells (maternal/fetal), trophoblasts, and other cells within the placenta are susceptible to immune suppression by the GBS hyaluronidase.

Although we observed relative suppression of inflammation at the maternal-fetal interface, fetal cytokines were induced in the setting of fetal bacteremia (Fig. 3). Given the *in vivo* and *in vitro* data obtained in this study, we propose that HylB may dampen proinflammatory cascades and microbicidal activity of first-line innate immune defenses such as neutrophils, thereby promoting bacterial replication and invasion of the amniotic cavity and fetus. We hypothesize that once bacteria have invaded the fetal niche, other proinflammatory, surface-associated bacterial factors (e.g., capsular polysaccharides [41], surface immunogenic protein [42], pilus [43]) overcome the immune-dampening effects of GBS HylB-digested HA fragments, triggering host PRRs and resulting in systemic fetal inflammation. A systemic fetal inflammatory response in GB37-infected fetuses may have

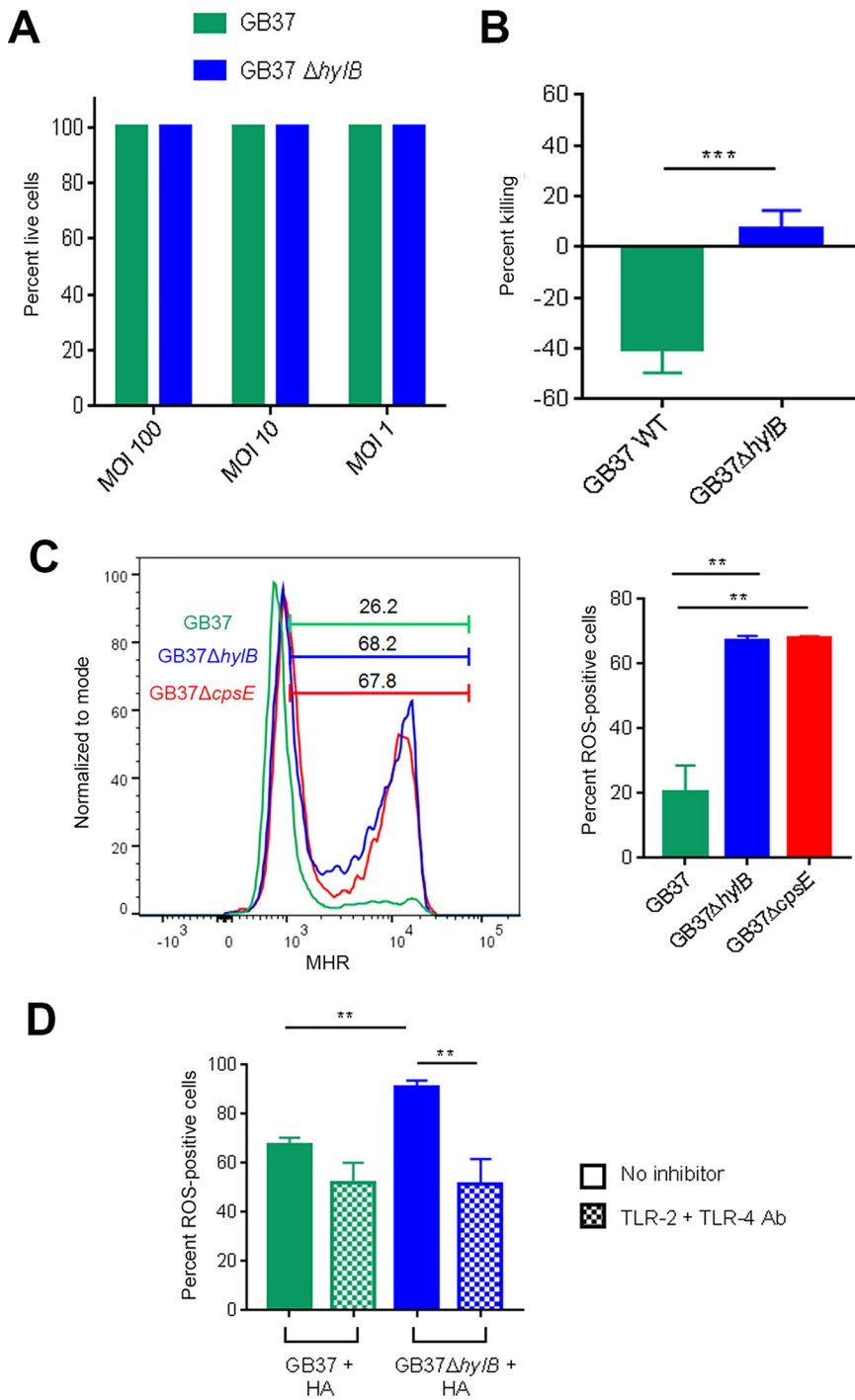


**FIG 6** GBS HylB evades neutrophil killing independently of cell death by interfering with TLR-2/4 signaling. (A) Primary human neutrophils were isolated from fresh adult blood, exposed to GB37 or GB37 $\Delta$ hylB at MOIs 100, 10, or 1 for 4 h, and then examined for cell death by LDH release. The percent live cells was calculated relative to Triton X-100-treated positive controls (0% live cells) and PBS-treated negative controls (100% live cells). (B) GB37 or GB37 $\Delta$ hylB was exposed to primary human neutrophils isolated from fresh blood (MOI of 1) for 1 h. The percent killing was calculated as the number of CFU recovered after incubation with neutrophils out of the number of the number CFU recovered after incubation without neutrophils  $\times$  100. Differences among groups were determined by a paired *t* test. (C) Primary human neutrophils were isolated as described above, pretreated with dihydrorhodamine-123 (DHR), and then exposed to GB37 or GB37 $\Delta$ hylB (MOI of 100). Since GBS capsule can suppress neutrophil ROS generation by blocking Siglec 9 (62), the GB37 $\Delta$ cpsE was included as a control. The conversion of DHR to fluorescent MHR indicates ROS production in cells and was measured by flow cytometry at 60 min postinfection. Differences

(Continued on next page)

triggered parturition in these animals, akin to fetal inflammatory response syndrome, which has been linked to preterm labor in humans (44, 45). Premature cervical softening is associated with increased MMP levels (Fig. 3) and prostaglandins, may have also played a role in early labor onset (46–48). Further research on the effect of HylB on host pathways during GBS infection is critical to understanding the multifaceted etiologies of GBS-associated preterm labor.

Limitations of our study include the lack of information on cellular events occurring in the amniotic fluid due to low cell recovery. In addition, we were unable to observe the cellular events at the placenta and uterus immediately after bacterial inoculation prior to preterm labor and delivery. Accordingly, it is possible that we did not capture events that may lend greater insight into the kinetics of GBS HylB-mediated immune suppression. For instance, as GB37 $\Delta$ hylB lacks the ability to degrade HA into anti-inflammatory dimers (21), GB37 $\Delta$ hylB inoculation may have induced rapid recruitment of neutrophils via controlled inflammation, resulting in swift clearance of this strain before microbial invasion of the amniotic cavity could occur (in all animals except GB37 $\Delta$ hylB#5). This idea is supported by our previous findings in an intraperitoneal murine model of infection, where we observed greater neutrophil recruitment to the peritoneal fluid of GB37 $\Delta$ hylB-inoculated mice within 2 h postinfection and less bacterial dissemination by 48 h compared to GB37-inoculated mice (29). In the present study, bacterial clearance and resolution of inflammation within the chorioamniotic membranes in four of five GB37 $\Delta$ hylB-treated NHPs could explain the lower neutrophil frequencies in the membranes and uterine tissues observed 3 days after inoculation. A time-controlled experiment in the NHP pregnancy model would lend greater insight into the differences in neutrophil recruitment and inflammatory events immediately following choriodecidual infection with GB37 or GB37 $\Delta$ hylB.

Together, our findings establish HylB as a potent virulence factor that allows GBS to circumvent neutrophil responses, invade the amniotic cavity, and cause fetal bacteremia and preterm labor in an animal model that closely resembles human pregnancy. The chronically catheterized model enabled us to evaluate uterine contraction patterns, cervical dilation, microbial invasion of the amniotic cavity, and amniotic fluid responses in real time, which is not possible in the pregnant mouse model. Data obtained from the NHP model show that the hyaluronidase-proficient WT GB37 strain induced significant uterine contraction leading to cervical dilation (similar to human preterm labor) as early as 6 h postinoculation and also significantly delayed and diminished placental, amniotic, uterine, and myometrial immune responses as seen via Luminex, flow cytometry, and digital spatial profiling. Accordingly, these results point to HylB as a potential therapeutic target for invasive GBS disease during pregnancy. Several known hyaluronidase inhibitors exist and have been proposed as therapeutics for other HA-mediated pathology, including sexually transmitted infections (49, 50), venom wounds (51, 52), and cancer (53–55). Identification of a HylB-specific inhibitor could lead to new treatments for GBS and have far-reaching impacts on maternal and neonatal health worldwide.

## MATERIALS AND METHODS

**Ethics statement.** Written informed patient consent for donation of adult human blood was obtained with approval from the Seattle Children's Research Institute Institutional Review Board (protocol 11117). Children under the age of 18 years were not recruited for donation of adult human blood for protocol 11117. Written informed patient consent for donation of maternal and cord blood was

### FIG 6 Legend (Continued)

among treatment groups were determined by one-way analysis of variance (ANOVA). (D) Filtered supernatants of stationary-phase GB37 or GB37 $\Delta$ hylB liquid cultures were incubated with HA for 18 h to allow for enzymatic digestion of HA. Meanwhile, primary human neutrophils were pretreated with 10  $\mu$ g/ml anti-TLR-2 antibody (Invivogen) plus 10  $\mu$ g/ml anti-TLR-4 antibody (Invivogen) or vehicle control. Neutrophils were treated with DHR and then exposed to the digested HA solutions from each strain for 60 min. As described above, ROS production in cells was measured by detecting fluorescent MHR via flow cytometry. Differences in MHR-positive cells among treatment groups were determined by one-way ANOVA. \*,  $P < 0.05$ ; \*\*,  $P < 0.01$ ; \*\*\*,  $P < 0.001$ ; \*\*\*\*,  $P < 0.0001$ ; ns,  $P \geq 0.05$ .

obtained from the University of Washington Institutional Review Board (protocol 34004). These studies were performed per the Principles in the WMA Declaration of Helsinki and Department of Health and Human Services Belmont Report.

All animal experiments were carried out in strict accordance with the recommendations in the *Guide for the Care and Use of Laboratory Animals* of the National Research Council and the Weatherall report, "The use of nonhuman primates in research." The protocol was approved by the University of Washington Institutional Animal Care and Use Committee (permit 4165-01). All surgery was performed under general anesthesia, and all efforts were made to minimize pain and distress.

**Chemicals.** Unless indicated otherwise, all chemicals were purchased from Sigma-Aldrich.

**Bacterial strains.** GBS strains used in the NHP model were derived from strain GB37 (serotype V, multilocus sequence type 1), which was isolated from the blood of a septic human neonate with early onset disease (56). This strain is neither hemolytic nor pigmented (57) but exhibits increased hyaluronidase activity compared to other GBS clinical isolates (29). The isogenic strain GB37 $\Delta$ *hylB* lacks hyaluronidase and was described previously (29). The GB37 $\Delta$ *cpsE* strain was derived from WT GB37 using methods described previously (22, 58) (see Text S1 for details). Cultures of GBS were grown in tryptic soy broth (TSB) or tryptic soy agar (TSA; Difco Laboratories) at 37°C with 5% CO<sub>2</sub>. For inoculations in the NHP model, GBS strains were grown to mid-log phase (OD<sub>600</sub> = 0.27), and 1 × 10<sup>8</sup> CFU in 1 ml of sterile PBS was inoculated into the choriodecidual space, as described below and previously (27, 28). Similarly, for *in vitro* studies, GBS strains were grown to mid-log phase (OD<sub>600</sub> = 0.27), washed, and resuspended in sterile phosphate-buffered saline (PBS) prior to infection unless otherwise noted.

**Chronically catheterized NHP model.** As described previously (28), pregnant pigtail macaques (*Macaca nemestrina*) were time-mated, and fetal age was determined using early ultrasound. Animals were provided drinking water at all times and fed commercial monkey chow, supplemented daily with fruits and vegetables. The temperature in the animal quarters was maintained between 72 and 82°F. Each animal was conditioned to a nylon jacket/tether system for several weeks before surgery, which allowed for free movement within the cage while protecting the catheters. Between days 116 and 125 of pregnancy (term = 172 days), NHPs were catheterized by laparotomic surgical implantation into the maternal femoral vein, amniotic cavity, and choriodecidual interface in the lower uterine segment (i.e., between the uterine muscle and fetal membranes, external to amniotic cavity). For detailed methods of catheterization surgery, see Text S1 in the supplemental material.

The experiment was initiated when a catheterized pregnant NHP received one of two experimental treatments: choriodecidual inoculation of either GBS strain GB37 (*n* = 5) or the isogenic strain GB37 $\Delta$ *hylB* (*n* = 5). Two chronically catheterized NHP that were inoculated with sterile saline were also included, along with four saline controls performed in previous studies (27, 59).

AF and maternal blood were collected for culture, cytokine, and prostaglandin analysis during each experiment. Intra-amniotic pressure was continuously recorded, digitized, and analyzed as described previously (27, 28). The integrated area under the curve for intrauterine pressure was used as a measure of uterine activity and reported as the hourly contraction area (HCA; mm Hg s<sup>2</sup> s/h) over 24 h. Preterm labor was defined as progressive cervical dilation associated with increased and sustained uterine activity (>10,000 mm Hg s<sup>2</sup> s/h). Cesarean section was performed at the following experimental endpoints to allow for tissue collection: (i) preterm labor, (ii) 3 days after GBS inoculation if preterm labor did not occur, or (iii) 7 days after saline inoculation (27, 28). After Cesarean section, fetuses were euthanized by barbiturate overdose, followed by exsanguination and fetal necropsy (27, 28). Complete gross and histopathologic examinations were performed. For details on sample collection, see Text S1 in the supplemental material.

**Placental and fetal lung histology.** A board-certified veterinary pathologist (A.B.) performed blinded histopathologic examination of the fetal and placental tissues. H&E-stained, full-thickness paraffin sections (placental disc, umbilical cord, and fetal membrane roll) were examined from each case to exclude inflammation, necrosis, fetal vascular thrombosis, or other histopathological findings. Chorioamnionitis was diagnosed by the presence of a neutrophilic infiltrate at the chorion-decidua junction (mild) or amniochorion junction (moderate or severe). For histologic examination of the fetal lung, two to three randomly selected fixed fetal lung tissues were embedded in paraffin, and sections were stained with H&E. We also performed immunostaining for MPO (a granulocyte marker) and CD68 (a macrophage marker) on the chorioamniotic membranes and fetal lung tissues (see Text S1 in the supplemental material).

**Digital spatial profiling.** GeoMx digital spatial profiling (DSP) was performed at NanoString Technologies in Seattle, WA. Formalin-fixed, paraffin-embedded placental sections from animals from each group were incubated with fluorescent probes and a multiplex cocktail of primary antibodies with photocleavable oligonucleotides (i.e., a validated DSP human-immune oncology protein panel; NanoString Technologies). The fluorescent markers included anti-pan cytokeratin-Alexa Fluor 488 (Pan-CK, clone AE1/AE3; Novusbio), anti-fibroblast activation protein-Alexa-Fluor 594 (FAP, clone SP325; Abcam), SYTO 83 for nuclei visualization (Thermo Fisher), and anti-GBS-Alexa Fluor 647 (clone ab53584; Abcam). Sections were magnified to 20×, and ROIs comprising the decidua, chorion, and amnion from each animal were selected based on tissue morphology (Fig. 5B). Each region of interest was then exposed to UV illumination with a double digital mirror device molecule, which cleaved the DNA oligonucleotides into the aqueous layer above the tissue slice. The oligonucleotides in the eluent were collected via microcapillary aspiration and transferred to an individual well of a microtiter plate. Oligonucleotides were then hybridized to nCounter optical barcodes (NanoString Technologies) to permit *ex situ* digital counting of each analyte. Briefly, hybridization of oligonucleotides to optical barcodes were performed at 65°C in a thermocycler. After hybridization, samples were processed using the nCounter prep station and digital analyzer. Data were normalized to technical controls and area. To generate signal/noise ratios, data were calculated relative to isotype controls.

**Neutrophil assays.** For detailed methods on neutrophil isolation from whole human blood, see the supplemental material. To measure neutrophil death, neutrophils ( $1 \times 10^5$  cells in RPMI containing L-glutamine) were exposed to GB37 or GB37 $\Delta$ hyfB (MOI of 100, 10, or 1) for 4 h at 37°C, and the release of LDH (lactate dehydrogenase) into cell supernatants was quantified using the LDH assay kit (TaKaRa) according to the manufacturer's instructions. The percent cell death was calculated relative to 0.1% Triton X-100-treated (100% cell death) and PBS-treated (0% cell death) controls. To measure neutrophil killing of GBS, neutrophils ( $1 \times 10^6$ ) were incubated with GB37 or GB37 $\Delta$ hyfB at an MOI of 1 in RPMI per g for 1 h at 37°C, as described previously (28, 60). Triton X-100 (0.1%) was added to lyse neutrophils and release intracellular bacteria, and total bacteria (intracellular and extracellular) were enumerated by serial dilution plating on TSA. The percent killing was calculated as the number of CFU recovered in the presence of neutrophils over the number of CFU recovered in the absence of neutrophils  $\times$  100. To measure ROS production, neutrophils ( $1 \times 10^6$  cells/ml in RPMI per g) were preincubated with 84  $\mu$ M dihydrorhodamine-123 (DHR; in 0.28% dimethyl sulfoxide) at 37°C for 20 min, as described previously (28), and then exposed to GB37, GB37 $\Delta$ hyfB, or GB37 $\Delta$ cpsE (MOI of 100) for 60 min. The fluorescence intensity of cells (which measures DHR oxidation by ROS to fluorescent MHR [monohydrorhodamine]) was measured immediately by flow cytometry using an LSR II (BD Biosciences). The data are representative of three experiments with neutrophils obtained from four independent donors. For details on treatment of neutrophils with anti-TLR-2/4 antibodies, please see the supplemental material. Data were analyzed using FlowJo v10.1 (FlowJo, LLC).

**Statistical analyses.** In all cases, results were considered significantly different if  $P < 0.05$ . However, because of the limited number of samples per group in NHP experiments, we also report  $P$  values between 0.05 and 0.100, as described previously for NHP experiments (28, 61). All statistical tests were unpaired and two-sided unless mentioned otherwise. For details on all statistical tests used in the study, see the supplemental material.

**Data availability.** All relevant data supporting the key findings of this study are available within the article and its supplemental material or from the corresponding authors upon request.

## SUPPLEMENTAL MATERIAL

Supplemental material is available online only.

**TEXT S1**, DOCX file, 0.04 MB.

**FIG S1**, DOCX file, 1.5 MB.

**FIG S2**, DOCX file, 0.9 MB.

**FIG S3**, DOCX file, 0.1 MB.

**FIG S4**, DOCX file, 0.4 MB.

**FIG S5**, DOCX file, 0.3 MB.

**FIG S6**, DOCX file, 0.3 MB.

**FIG S7**, DOCX file, 0.3 MB.

**FIG S8**, DOCX file, 0.1 MB.

**TABLE S1**, DOCX file, 0.02 MB.

## ACKNOWLEDGMENTS

We thank Shannon Manning for providing the GB37 strain and Connie Hughes for administrative support.

This study was supported by funding from the National Institutes of Health grants R01AI133976, R01AI100989, R01AI145890, and R01AI112619 to L.R. and K.M.A.W., and seed funds from Seattle Children's Research Institute to L.R. NIH training grant T32AI007509 (principal investigator [PI] Lee Ann Campbell) supported J.V. and A.B., and T32AI055396 (PI Ferric Fang) supported A.F. The content is solely the responsibility of the authors and does not necessarily represent the official views of the National Institutes of Health.

L.R., K.M.A.W., M.C., B.A., C.G., and J.V. designed the experiments. M.C., B.A., A.O., P.Q., A.B., C.G., K.S., J.O., S.M., M.D., T-Y.W., A.B., A.F., S.N., K.M.A.W., and L.R. performed the experiments. M.C., B.A., A.O., P.Q., C.G., S.M., M.D., T-Y.W., J.M., A.B., A.F., K.M.A.W., and L.R. analyzed the results, and B.A., M.C., K.M.A.W., and L.R. wrote the manuscript.

We declare there are no conflicts of interest.

## REFERENCES

1. Institute of Medicine. 2007. In Behrman RE, Butler AS (ed), Preterm birth: causes, consequences, and prevention. Institute of Medicine, Washington, DC. <https://doi.org/10.17226/11622>.
2. Goldenberg RL, Hauth JC, Andrews WW. 2000. Intrauterine infection and preterm delivery. *N Engl J Med* 342:1500–1507. <https://doi.org/10.1056/NEJM200005183422007>.
3. Hillier SL, Krohn MA, Kiviat NB, Watts DH, Eschenbach DA. 1991. Microbiologic causes and neonatal outcomes associated with chorioamnion



- infection. *Am J Obstet Gynecol* 165:955–961. [https://doi.org/10.1016/0002-9378\(91\)90447-y](https://doi.org/10.1016/0002-9378(91)90447-y).
4. Campbell JR, Hillier SL, Krohn MA, Ferrieri P, Zaleznik DF, Baker CJ. 2000. Group B streptococcal colonization and serotype-specific immunity in pregnant women at delivery. *Obstet Gynecol* 96:498–503.
  5. Brigtsen AK, Jacobsen AF, Dedi L, Melby KK, Fugelseth D, Whitelaw A. 2015. Maternal colonization with group B *Streptococcus* is associated with an increased rate of infants transferred to the neonatal intensive care unit. *Neonatology* 108:157–163. <https://doi.org/10.1159/000434716>.
  6. Bianchi-Jassir F, Seale AC, Kohli-Lynch M, Lawn JE, Baker CJ, Bartlett L, Cutland C, Gravett MG, Heath PT, Ip M, Le Doare K, Madhi SA, Saha SK, Schrag S, Sobanjo-Ter Meulen A, Vekemans J, Rubens CE. 2017. Preterm birth associated with group B streptococcus maternal colonization worldwide: systematic review and meta-analyses. *Clin Infect Dis* 65:S133–S142. <https://doi.org/10.1093/cid/cix661>.
  7. Seale AC, Bianchi-Jassir F, Russell NJ, Kohli-Lynch M, Tann CJ, Hall J, Madrid L, Blencowe H, Cousens S, Baker CJ, Bartlett L, Cutland C, Gravett MG, Heath PT, Ip M, Le Doare K, Madhi SA, Rubens CE, Saha SK, Schrag SJ, Sobanjo-Ter Meulen A, Vekemans J, Lawn JE. 2017. Estimates of the burden of group B streptococcal disease worldwide for pregnant women, stillbirths, and children. *Clin Infect Dis* 65:S200–S219. <https://doi.org/10.1093/cid/cix664>.
  8. Schrag SJ, Zywicki S, Farley MM, Reingold AL, Harrison LH, Lefkowitz LB, Hadler JL, Danila R, Cieslak PR, Schuchat A. 2000. Group B streptococcal disease in the era of intrapartum antibiotic prophylaxis. *N Engl J Med* 342:15–20. <https://doi.org/10.1056/NEJM200001063420103>.
  9. Centers for Disease Control and Prevention. 2007. Perinatal group B streptococcal disease after universal screening recommendations—United States, 2003–2005. *MMWR Morb Mortal Wkly Rep* 56:701–705.
  10. Verani JR, McGee L, Schrag SJ. 2010. Prevention of perinatal group B streptococcal disease—revised guidelines from CDC, 2010. *MMWR Recomm Rep* 59:1–36.
  11. Rivera L, Saez-Llorens X, Feris-Iglesias J, Ip M, Saha S, Adrian PV, Madhi SA, Boudville IC, Cunningham MC, Casellas JM, Slobod KS. 2015. Incidence and serotype distribution of invasive group B streptococcal disease in young infants: a multi-country observational study. *BMC Pediatr* 15:143. <https://doi.org/10.1186/s12887-015-0460-2>.
  12. Berardi A, Cattelan C, Creti R, Berner R, Pietrangiolillo Z, Margarit I, Maione D, Ferrari F. 2015. Group B streptococcal infections in the newborn infant and the potential value of maternal vaccination. *Expert Rev Anti Infect Ther* 13:1387–1399. <https://doi.org/10.1586/14787210.2015.1079126>.
  13. Stern R, Jedrzejak MJ. 2006. Hyaluronidases: their genomics, structures, and mechanisms of action. *Chem Rev* 106:818–839. <https://doi.org/10.1021/cr050247k>.
  14. Fallacara A, Baldini E, Manfredini S, Vertuani S. 2018. Hyaluronic acid in the third millennium. *Polymers (Basel)* 10:701. <https://doi.org/10.3390/polym10070701>.
  15. Litwiniuk M, Krejner A, Speyrer MS, Gauto AR, Grzela T. 2016. Hyaluronic acid in inflammation and tissue regeneration. *Wounds* 28:78–88.
  16. Jiang D, Liang J, Fan J, Yu S, Chen S, Luo Y, Prestwich GD, Mascarenhas MM, Garg HG, Quinn DA, Homer RJ, Goldstein DR, Bucala R, Lee PJ, Medzhitov R, Noble PW. 2005. Regulation of lung injury and repair by Toll-like receptors and hyaluronan. *Nat Med* 11:1173–1179. <https://doi.org/10.1038/nm1315>.
  17. Hynes WL, Walton SL. 2000. Hyaluronidases of Gram-positive bacteria. *FEMS Microbiol Lett* 183:201–207. <https://doi.org/10.1111/j.1574-6968.2000.tb08958.x>.
  18. Wang Z, Guo C, Xu Y, Liu G, Lu C, Liu Y. 2014. Two novel functions of hyaluronidase from *Streptococcus agalactiae* are enhanced intracellular survival and inhibition of proinflammatory cytokine expression. *Infect Immun* 82:2615–2625. <https://doi.org/10.1128/IAI.00022-14>.
  19. Gochnauer TA, Wilson JB. 1951. Hyaluronidase production *in vitro* by streptococci isolated from bovine mastitis cases. *Am J Vet Res* 12:20–22.
  20. Pritchard DG, Lin B, Willingham TR, Baker JR. 1994. Characterization of the group B streptococcal hyaluronate lyase. *Arch Biochem Biophys* 315:431–437. <https://doi.org/10.1006/abbi.1994.1521>.
  21. Kolar SL, Kyme P, Tseng CW, Soliman A, Kaplan A, Liang J, Nizet V, Jiang D, Murali R, Arditi M, Underhill DM, Liu GY. 2015. Group B *Streptococcus* evades host immunity by degrading hyaluronan. *Cell Host Microbe* 18:694–704. <https://doi.org/10.1016/j.chom.2015.11.001>.
  22. Vornhagen J, Quach P, Boldenow E, Merillat S, Whidbey C, Ngo LY, Adams Waldorf KM, Rajagopal L. 2016. Bacterial hyaluronidase promotes ascending GBS infection and preterm birth. *mBio* 7:e00781–16. <https://doi.org/10.1128/mBio.00781-16>.
  23. Mitchell BF, Taggart MJ. 2009. Are animal models relevant to key aspects of human parturition? *Am J Physiol Regul Integr Comp Physiol* 297:R525–R545. <https://doi.org/10.1152/ajpregu.00153.2009>.
  24. Carter AM. 2007. Animal models of human placentation: a review. *Placenta* 28(Suppl A):S41–S47. <https://doi.org/10.1016/j.placenta.2006.11.002>.
  25. Adams Waldorf KM, Rubens CE, Gravett MG. 2011. Use of nonhuman primate models to investigate mechanisms of infection-associated preterm birth. *BJOG* 118:136–144. <https://doi.org/10.1111/j.1471-0528.2010.02728.x>.
  26. Gravett MG, Witkin SS, Haluska GJ, Edwards JL, Cook MJ, Novy MJ. 1994. An experimental model for intraamniotic infection and preterm labor in rhesus monkeys. *Am J Obstet Gynecol* 171:1660–1667. [https://doi.org/10.1016/0002-9378\(94\)90418-9](https://doi.org/10.1016/0002-9378(94)90418-9).
  27. Adams Waldorf KM, Gravett MG, McAdams RM, Paoletta LJ, Gough GM, Carl DJ, Bansal A, Liggitt HD, Kapur RP, Reitz FB, Rubens CE. 2011. Chorio-decidual group B streptococcal inoculation induces fetal lung injury without intra-amniotic infection and preterm labor in Macaca nemestrina. *PLoS One* 6:e28972. <https://doi.org/10.1371/journal.pone.0028972>.
  28. Boldenow E, Gendrin C, Ngo L, Bierle C, Vornhagen J, Coleman M, Merillat S, Armistead B, Whidbey C, Alishetti V, Santana-Ufret V, Ogle J, Gough M, Srinouanprachanh S, MacDonald JW, Bammler TK, Bansal A, Liggitt HD, Rajagopal L, Adams Waldorf KM. 2016. Group B *Streptococcus* circumvents neutrophils and neutrophil extracellular traps during amniotic cavity invasion and preterm labor. *Sci Immunol* 1:eaa4576.
  29. Gendrin C, Vornhagen J, Armistead B, Singh P, Whidbey C, Merillat S, Knupp D, Parker R, Rogers LM, Quach P, Iyer LM, Aravind L, Manning SD, Aronoff DM, Rajagopal L. 2018. A nonhemolytic group B streptococcus strain exhibits hypervirulence. *J Infect Dis* 217:983–987. <https://doi.org/10.1093/infdis/jix646>.
  30. Geng J, Huang C, Jiang S. 2016. Roles and regulation of the matrix metalloproteinase system in parturition. *Mol Reprod Dev* 83:276–286. <https://doi.org/10.1002/mrd.22626>.
  31. Lombardi A, Makieva S, Rinaldi SF, Arcuri F, Petraglia F, Norman JE. 2018. Expression of matrix metalloproteinases in the mouse uterus and human myometrium during pregnancy, labor, and preterm labor. *Reprod Sci* 25:938–949. <https://doi.org/10.1177/1933719117732158>.
  32. Ravanos K, Dagklis T, Petousis S, Margioulas-Siarkou C, Prapas Y, Prapas N. 2015. Factors implicated in the initiation of human parturition in term and preterm labor: a review. *Gynecol Endocrinol* 31:679–683. <https://doi.org/10.3109/09513590.2015.1076783>.
  33. Lee SM, Park KH, Jung EY, Cho SH, Ryu A. 2016. Prediction of spontaneous preterm birth in women with cervical insufficiency: comprehensive analysis of multiple proteins in amniotic fluid. *J Obstet Gynaecol Res* 42:776–783. <https://doi.org/10.1111/jog.12976>.
  34. Vadillo-Ortega F, Estrada-Gutierrez G. 2005. Role of matrix metalloproteinases in preterm labour. *BJOG* 112(Suppl 1):19–22. <https://doi.org/10.1111/j.1471-0528.2005.00579.x>.
  35. Sundrani DP, Chavan-Gautam PM, Pisal HR, Mehendale SS, Joshi SR. 2012. Matrix metalloproteinase-1 and -9 in human placenta during spontaneous vaginal delivery and caesarean sectioning in preterm pregnancy. *PLoS One* 7:e29855. <https://doi.org/10.1371/journal.pone.0029855>.
  36. Lin J, Haridas S, Barenkamp SJ, Lorenset LC, Lee ASE, Schroeder BT, Peng G, Koenig JM. 2018. Neonatal neutrophils stimulated by group B *Streptococcus* induce a proinflammatory T-helper cell bias. *Pediatr Res* 83:739–746. <https://doi.org/10.1038/pr.2017.272>.
  37. Rouschop KM, Roelofs JJ, Claessen N, da Costa Martins P, Zwaginga JJ, Pals ST, Weening JJ, Florquin S. 2005. Protection against renal ischemia reperfusion injury by CD44 disruption. *J Am Soc Nephrol* 16:2034–2043. <https://doi.org/10.1681/ASN.2005010054>.
  38. Koga K, Mor G. 2010. Toll-like receptors at the maternal-fetal interface in normal pregnancy and pregnancy disorders. *Am J Reprod Immunol* 63:587–600. <https://doi.org/10.1111/j.1600-0897.2010.00848.x>.
  39. Ma Y, Mor G, Abrahams VM, Buhimschi IA, Buhimschi CS, Guller S. 2006. Alterations in syncytiotrophoblast cytokine expression following treatment with lipopolysaccharide. *Am J Reprod Immunol* 55:12–18. <https://doi.org/10.1111/j.1600-0897.2005.00347.x>.
  40. Adams KM, Lucas J, Kapur RP, Stevens AM. 2007. LPS induces translocation of TLR4 in amniotic epithelium. *Placenta* 28:477–481. <https://doi.org/10.1016/j.placenta.2006.08.004>.
  41. von Hunolstein C, Totolian A, Alfaroni G, Mancuso G, Cusumano V, Teti G, Orefici G. 1997. Soluble antigens from group B streptococci induce

- cytokine production in human blood cultures. *Infect Immun* 65:4017–4021. <https://doi.org/10.1128/IAI.65.10.4017-4021.1997>.
42. Diaz-Dinamarca DA, Manzo RA, Soto DA, Avendano-Valenzuela MJ, Bastias DN, Soto PI, Escobar DF, Vasquez-Saez V, Carrion F, Pizarro-Ortega MS, Wilson CAM, Berrios J, Kalergis AM, Vasquez AE. 2020. Surface immunogenic protein of streptococcus group B is an agonist of Toll-like receptors 2 and 4 and a potential immune adjuvant. *Vaccines (Basel)* 8:29. <https://doi.org/10.3390/vaccines8010029>.
  43. Banerjee A, Kim BJ, Carmona EM, Cutting AS, Gurney MA, Carlos C, Feuer R, Prasadarao NV, Doran KS. 2011. Bacterial pili exploit integrin machinery to promote immune activation and efficient blood-brain barrier penetration. *Nat Commun* 2:462. <https://doi.org/10.1038/ncomms1474>.
  44. Romero R, Gomez R, Ghezzi F, Yoon BH, Mazor M, Edwin SS, Berry SM. 1998. A fetal systemic inflammatory response is followed by the spontaneous onset of preterm parturition. *Am J Obstet Gynecol* 179:186–193. [https://doi.org/10.1016/S0002-9378\(98\)70271-6](https://doi.org/10.1016/S0002-9378(98)70271-6).
  45. Gomez R, Romero R, Ghezzi F, Yoon BH, Mazor M, Berry SM. 1998. The fetal inflammatory response syndrome. *Am J Obstet Gynecol* 179:194–202. [https://doi.org/10.1016/S0002-9378\(98\)70272-8](https://doi.org/10.1016/S0002-9378(98)70272-8).
  46. Ekerhovd E, Weijdegard B, Brannstrom M, Mattsby-Baltzer I, Norstrom A. 2002. Nitric oxide induced cervical ripening in the human: involvement of cyclic guanosine monophosphate, prostaglandin F<sub>2α</sub>, and prostaglandin E<sub>2</sub>. *Am J Obstet Gynecol* 186:745–750. <https://doi.org/10.1067/mob.2002.121327>.
  47. El Maradny E, Kanayama N, Kobayashi H, Hossain B, Khatun S, Liping S, Kobayashi T, Terao T. 1997. The role of hyaluronic acid as a mediator and regulator of cervical ripening. *Hum Reprod* 12:1080–1088. <https://doi.org/10.1093/humrep/12.5.1080>.
  48. Mahendroo M. 2019. Cervical hyaluronan biology in pregnancy, parturition and preterm birth. *Matrix Biol* 78–79:24–31. <https://doi.org/10.1016/j.matbio.2018.03.002>.
  49. Anderson RA, Feathergill K, Diao X, Cooper M, Kirkpatrick R, Spear P, Waller DP, Chany C, Doncel GF, Herold B, Zaneveld LJ. 2000. Evaluation of poly(styrene-4-sulfonate) as a preventive agent for conception and sexually transmitted diseases. *J Androl* 21:862–875.
  50. Zaneveld LJ, Waller DP, Anderson RA, Chany C, II, Rencher WF, Feathergill K, Diao XH, Doncel GF, Herold B, Cooper M. 2002. Efficacy and safety of a new vaginal contraceptive antimicrobial formulation containing high molecular weight poly(sodium 4-styrenesulfonate). *Biol Reprod* 66:886–894. <https://doi.org/10.1095/biolreprod66.4.886>.
  51. Kemparaju K, Girish KS. 2006. Snake venom hyaluronidase: a therapeutic target. *Cell Biochem Funct* 24:7–12. <https://doi.org/10.1002/cbf.1261>.
  52. Oliveira-Mendes BBR, Miranda SEM, Sales-Medina DF, Magalhaes BF, Kalapothakis Y, Souza RP, Cardoso VN, de Barros ALB, Guerra-Duarte C, Kalapothakis E, Horta CCR. 2019. Inhibition of *Tityus serrulatus* venom hyaluronidase affects venom biodistribution. *PLoS Negl Trop Dis* 13:e0007048. <https://doi.org/10.1371/journal.pntd.0007048>.
  53. Botzki A, Rigden DJ, Braun S, Nukui M, Salmen S, Hoechstetter J, Bernhardt G, Dove S, Jedrzejewski MJ, Buschauer A. 2004. L-Ascorbic acid 6-hexadecanoate, a potent hyaluronidase inhibitor. X-ray structure and molecular modeling of enzyme-inhibitor complexes. *J Biol Chem* 279:45990–45997. <https://doi.org/10.1074/jbc.M406146200>.
  54. Girish KS, Kemparaju K. 2007. The magic glue hyaluronan and its eraser hyaluronidase: a biological overview. *Life Sci* 80:1921–1943. <https://doi.org/10.1016/j.lfs.2007.02.037>.
  55. Girish KS, Kemparaju K, Nagaraju S, Vishwanath BS. 2009. Hyaluronidase inhibitors: a biological and therapeutic perspective. *Curr Med Chem* 16:2261–2288. <https://doi.org/10.2174/092986709788453078>.
  56. Davies HD, Adair C, McGeer A, Ma D, Robertson S, Mucenski M, Kowalsky L, Tyrell G, Baker CJ. 2001. Antibodies to capsular polysaccharides of group B *Streptococcus* in pregnant Canadian women: relationship to colonization status and infection in the neonate. *J Infect Dis* 184:285–291. <https://doi.org/10.1086/322029>.
  57. Singh P, Aronoff DM, Davies HD, Manning SD. 2016. Draft genome sequence of an invasive *Streptococcus agalactiae* isolate lacking pigmentation. *Genome Announc* 4:e00015-16.
  58. Rajagopal L, Clancy A, Rubens CE. 2003. A eukaryotic type serine/threonine kinase and phosphatase in *Streptococcus agalactiae* reversibly phosphorylate an inorganic pyrophosphatase and affect growth, cell segregation, and virulence. *J Biol Chem* 278:14429–14441. <https://doi.org/10.1074/jbc.M212747200>.
  59. Adams Waldorf KM, Singh N, Mohan AR, Young RC, Ngo L, Das A, Tsai J, Bansal A, Paoletta L, Herbert BR, Sooranna SR, Gough GM, Astley C, Vogel K, Baldessari AE, Bammler TK, MacDonald J, Gravett MG, Rajagopal L, Johnson MR. 2015. Uterine overdistention induces preterm labor mediated by inflammation: observations in pregnant women and nonhuman primates. *Am J Obstet Gynecol* 213:830e1–830e19. <https://doi.org/10.1016/j.ajog.2015.08.028>.
  60. Maisey HC, Quach D, Hensler ME, Liu GY, Gallo RL, Nizet V, Doran KS. 2008. A group B streptococcal pilus protein promotes phagocyte resistance and systemic virulence. *FASEB J* 22:1715–1724. <https://doi.org/10.1096/fj.07-093963>.
  61. Rueda CM, Presicce P, Jackson CM, Miller LA, Kallapur SG, Jobe AH, Choungnet CA. 2016. Lipopolysaccharide-induced chorioamnionitis promotes IL-1-dependent inflammatory FOXP3<sup>+</sup> CD4<sup>+</sup> T cells in the fetal rhesus macaque. *J Immunol* 196:3706–3715. <https://doi.org/10.4049/jimmunol.1502613>.
  62. Secundino I, Lizcano A, Roupe KM, Wang X, Cole JN, Olson J, Ali SR, Dahesh S, Amayreh LK, Henningham A, Varki A, Nizet V. 2016. Host and pathogen hyaluronan signal through human siglec-9 to suppress neutrophil activation. *J Mol Med* 94:219–233. <https://doi.org/10.1007/s00109-015-1341-8>.